Structural Basis for the Inhibition of Firefly Luciferase by a General Anesthetic

N. P. Franks, A. Jenkins, E. Conti, W. R. Lieb, and P. Brick
Biophysics Section, The Blackett Laboratory, Imperial College of Science, Technology and Medicine, London, England

ABSTRACT The firefly luciferase enzyme from *Photinus pyralis* is probably the best-characterized model system for studying anesthetic-protein interactions. It binds a diverse range of general anesthetics over a large potency range, displays a sensitivity to anesthetics that is very similar to that found in animals, and has an anesthetic sensitivity that can be modulated by one of its substrates (ATP). In this paper we describe the properties of bromoform acting as a general anesthetic (in *Rana temporaria* tadpoles) and as an inhibitor of the firefly luciferase enzyme at high and low ATP concentrations. In addition, we describe the crystal structure of the low-ATP form of the luciferase enzyme in the presence of bromoform at 2.2-Å resolution. These results provide a structural basis for understanding the anesthetic inhibition of the enzyme, as well as an explanation for the ATP modulation of its anesthetic sensitivity.

INTRODUCTION

Despite a growing appreciation that the effects of general anesthetics can be accounted for in terms of their direct interactions with proteins (Forman et al., 1995; Franks and Lieb, 1982, 1994; Mihic et al., 1997), there is remarkably little information available on the nature or molecular architectures of their binding sites (see Miller (1985) for a review). Some information has been gleaned from correlations of anesthetic potency with partitioning into defined solvents (Abraham et al., 1991; Franks and Lieb, 1978; Hansch et al., 1975; Taheri et al., 1991); however, this is an approach that can only give a picture of an "average" anesthetic-binding environment. What has emerged from these studies is a site that is predominantly hydrophobic, or apolar, but with a distinct polar component. The polar aspect of anesthetic binding sites has been stressed by several workers (Abraham et al., 1991; Franks and Lieb, 1978; Sandorfy, 1978), with an additional recent refinement that this polar component appears to act as a good hydrogen bond acceptor, but a poor donor (Abraham et al., 1991). Apart from the pioneering studies of Schoenborn and his colleagues on the binding of anesthetics to hemoglobin and myoglobin (Schoenborn, 1976; Schoenborn et al., 1965), detailed structural information on anesthetic-protein interactions has been lacking; this information can only be provided by techniques such as x-ray crystallography.

Recently in this laboratory we have determined (Conti et al., 1996a) the crystal structure of what is probably the best-characterized model of an anesthetic target, the firefly luciferase enzyme. This soluble enzyme has been shown to be inhibited by a diverse range of general anesthetics with a sensitivity that closely parallels anesthetic potencies in animals over five orders of magnitude (Franks and Lieb, 1984). In addition, the circumscribed dimensions and amphiphilic nature of the anesthetic-binding site on the luciferase enzyme provide a plausible explanation (Franks and Lieb, 1985) for the abrupt "cutoff" in potency that is found in homologous series of long-chain compounds. Furthermore, the observation that high concentrations of one of its substrates (ATP) trigger a conformational change in the enzyme that enhances anesthetic binding (Moss et al., 1991) provides added interest in the structure. This is because an analogous behavior is found with several ion channel receptors, such as the $GABA_A$, glycine, and $5\text{-}HT_3$ receptors. With these ligand-gated ion channels, volatile anesthetics enhance the apparent binding of the neurotransmitter, which, as we have recently pointed out (Tomlin et al., 1998), means that high concentrations of neurotransmitter must in turn enhance the binding of anesthetics.

For all of these reasons, the high-resolution structure of the firefly luciferase enzyme in the presence and absence of general anesthetics is of considerable interest. In this paper we report our first results using the simple achiral anesthetic bromoform binding to the enzyme in the absence of ATP, and we correlate our crystallographic analysis of the structure with the effects of bromoform on the activity of the enzyme and as a general anesthetic in animals.

MATERIALS AND METHODS

Anesthetic potency measurements in tadpoles

The general anesthetic potency of bromoform was determined for 4–6-week-old *Rana temporaria* tadpoles (Blades Biological Ltd., Cowden, Kent, England) in the pre-limb-bud stage of development (average length ~2 cm). Tadpoles were maintained in an aerated aquarium at 20–22°C. During randomized blind anesthetic potency experiments, 10 tadpoles were placed in each of a number of beakers containing 300 ml of tap water (20 ±

Received for publication 20 April 1998 and in final form 14 July 1998.

Address reprint requests to Dr. N. P. Franks, Biophysics Section, The Blackett Laboratory, Imperial College, Prince Consort Rd., London SW7 2BZ, England. Tel.: 44-171-594-7629; Fax: 44-171-589-0191; E-mail: n.franks@ic.ac.uk.

Dr. Conti's present address is Laboratory of Molecular Biophysics, Rockefeller University, New York, NY 10021.

Dr. Jenkins' present address is Department of Anesthesia and Critical Care, University of Chicago, Chicago, IL 60637.

0006-3495/98/11/2205/07 $2.00

1°C), with or without bromoform. The anesthetic end point was defined as the lack of a purposeful and sustained swimming response after a gentle inversion with a smooth glass rod. The number of anesthetized tadpoles was recorded every 10 min for 120 min (equilibrium was complete at 10–20 min), after which the tadpoles were returned to fresh tap water, where recovery was monitored. In all cases, normal swimming activity was restored within 30 min. Tadpole concentration-response data were fitted according to the method of Waud (1972) to a logistic equation of the form

$$p = \frac{100I^n}{I^n + (EC_{50})^n} \quad (1)$$

where p is the percentage of the population anesthetized, I is the bromoform concentration, n is the slope, and EC_{50} is the bromoform concentration for a half-maximum effect.

Anesthetic inhibition measurements of firefly luciferase

The luciferase enzyme from the North American firefly *Photinus pyralis* was obtained from Promega (Southampton, England) as a 61-kDa recombinant monomeric protein. HEPPS (*N*-(2-hydroxyethyl)-piperazine-*N*′-(3-propanesulfonic acid)) and ATP (disodium salt, grade I) were purchased from Sigma Chemical Company (Poole, Dorset, England), and D-luciferin was obtained from Europa Research Products (Ely, Cambridgeshire, England). $MgSO_4$ (Analar grade) was obtained from BDH (Poole, Dorset, England), and bromoform was from either Sigma Chemical Company or BDH.

Firefly luciferase combines with its substrate luciferin in the presence of ATP, Mg^{2+}, and O_2 to give a photon of light (McElroy and Seliger, 1961). Luciferase activity and its inhibition by bromoform were determined (Franks and Lieb, 1984) from the peak light output observed after 2.5 ml of a buffered ATP solution was rapidly injected into a reaction vial containing 5 ml of a buffered solution containing the luciferase enzyme, its natural substrate firefly luciferin, $MgSO_4$, and anesthetic (when appropriate). See Dickinson et al. (1993) for further details. The buffer was 25 mM HEPPS, titrated to pH 7.8 at 20°C with NaOH. Final concentrations were 2 mM or 2 μM ATP, 6.67 mM $MgSO_4$, 2–1800 μM luciferin, and 3 nM luciferase. Bromoform was added to the reaction vial in aliquots of a saturated aqueous solution (taken to be 11.9 mM; IARC, 1991).

Enzyme inhibition is expressed as the ratio of the control peak height v_o to the peak height in the presence of anesthetic v and plotted as a function of the anesthetic concentration I. Curves were fitted through these data using the method of weighted least squares, with weights (derived by assuming a constant percentage error in the measurement of enzyme activity) proportional to $(v/v_o)^2$. When the data are plotted as $\sqrt{v_0/v}$, straight lines were fitted with weights proportional to v/v_o.

X-ray crystallography

Crystals of recombinant firefly luciferase belonging to space group $P4_12_12$ with cell dimensions $a = b = 119.6$ Å, $c = 95.8$ Å, were obtained as previously described (Conti et al., 1996b), using the microbatch technique. The crystals were harvested and soaked for 5 min in a solution containing 16% w/v PEG 8000, 5% glycerol, 12.5% ethylene glycol, 100 mM Li_2SO_4, and 60 mM Tris HCl (pH 7.8) with saturating bromoform and then transferred and soaked for 2 min in a cryoprotectant solution, also saturated with bromoform containing 8% w/v PEG 8000, 10% glycerol, 12.5% ethylene glycol, and 100 mM Tris HCl (pH 7.8). Crystals were frozen in a stream of nitrogen gas at 100 K, and diffraction data to 2.2-Å resolution were recorded on a MarResearch (Hamburg, Germany) image plate detector using radiation produced by the synchrotron radiation source at Daresbury (England). The images were evaluated with the program MOSFLM (Andrew Leslie, unpublished), and the data were reduced using the CCP4 program suite (CCP4, 1994). Starting with the coordinates obtained for the unliganded luciferase molecule (Conti et al., 1996a), the structure was refined with the program X-plor (Brünger et al., 1987). Details of the data collection and refinement are presented in Table 1. The coordinates have been deposited with the Protein Data Bank (accession identifier: 1BA3).

RESULTS

We determined the potency of bromoform for producing a loss of righting reflex in tadpoles (*Rana temporaria*). We found that concentrations of bromoform in excess of ~100 μM rapidly (~15 min) induced a reversible state of loss of righting reflex and that the concentration-response curve could be fitted by a logistic equation (see Materials and Methods, Eq. 1) with an EC_{50} of 185 ± 3 μM bromoform and a slope $n = 8.2 \pm 0.5$ (see Fig. 1).

We studied the effects of bromoform on the firefly luciferase enzyme at both high (2 mM) and low (2 μM) concentrations of ATP because we (Moss et al., 1991) have previously found that ATP can modulate the anesthetic sensitivity of the enzyme, with luciferase being more sensitive at high ATP concentrations. We found a similar behavior here, with the peak light output being more sensitive to bromoform at the higher ATP concentration (see Fig. 2, *A* and *B*). In both cases, however, the inhibition increased quadratically and $\sqrt{v_0/v}$ increased linearly with bromoform concentration, indicating that two molecules of the anesthetic were involved in the inhibition of the enzyme.

We investigated the mechanism of bromoform inhibition at low concentrations of ATP and found it to be largely competitive (with respect to the substrate luciferin) in nature. This can be seen from the double-reciprocal plot of activity versus luciferin concentration in Fig. 3, which shows that the control and inhibited lines come close to intersecting on the ordinate axis (Fig. 3, *dashed line*) but have very different intersections on the abscissa axis. Even at the high concentration of 1600 μM bromoform, the effect on the maximum rate of the reaction V_{max} was small (~23%

TABLE 1 Crystallographic statistics

Synchrotron	Daresbury
Beam line	SRS 9.5
Wavelength	0.87 Å
Resolution range	18.4–2.2 Å
Measured reflections	109,681
Unique reflections	35,038
R_{merge}*	7.1 (23.5)%#
Completeness	98.2 (97.9)%#
Refinement	
R_{factor}§	19.7%
R_{free}¶	23.9%
Rms deviation from ideal bond lengths	0.007 Å
Rms deviation from ideal bond angles	1.51°

*$R_{merge} = 100 \times \Sigma_h \Sigma_j |I_{hj} - I_h| / \Sigma_h \Sigma_j I_{hj}$, where I_h is the weighted mean intensity of the symmetry related reflections I_{hj}.

#Values for the outermost resolution shell are given in parentheses.

§$R_{factor} = 100 \times \Sigma |F_{obs} - F_{calc}| / \Sigma |F_{obs}|$, where F_{obs} and F_{calc} are the observed and calculated structure factors, respectively.

¶R_{free} is the R_{factor} calculated using a random 5% sample of reflection data omitted from refinement (Brünger, 1992).

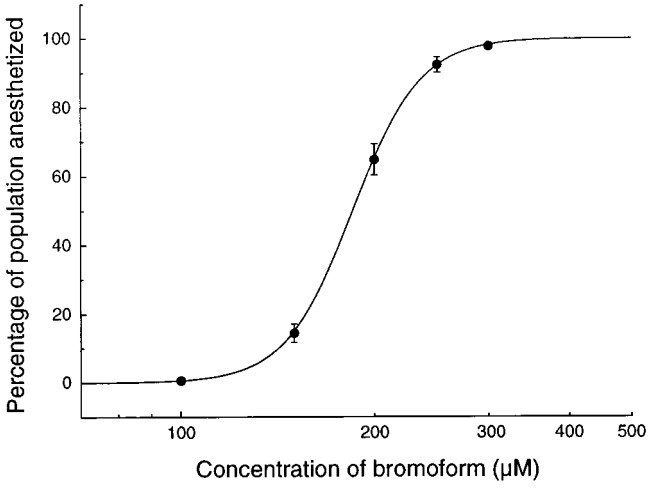

FIGURE 1 Concentration-response data for loss of righting reflex in tadpoles (*Rana temporaria*) for bromoform. Each data point (●) represents the mean response for an average of nine tadpoles. The line is a best fit to a logistic function defined by Waud (1972) for the analysis of quantal concentration-response curves (see Materials and Methods, Eq. 1). The error bars are standard errors of the mean. Where error bars are not shown they are smaller than the symbol. The best fit gave $EC_{50} = 185 \pm 3$ μM and slope $n = 8.2 \pm 0.5$. Note that the abscissa is on a logarithmic scale.

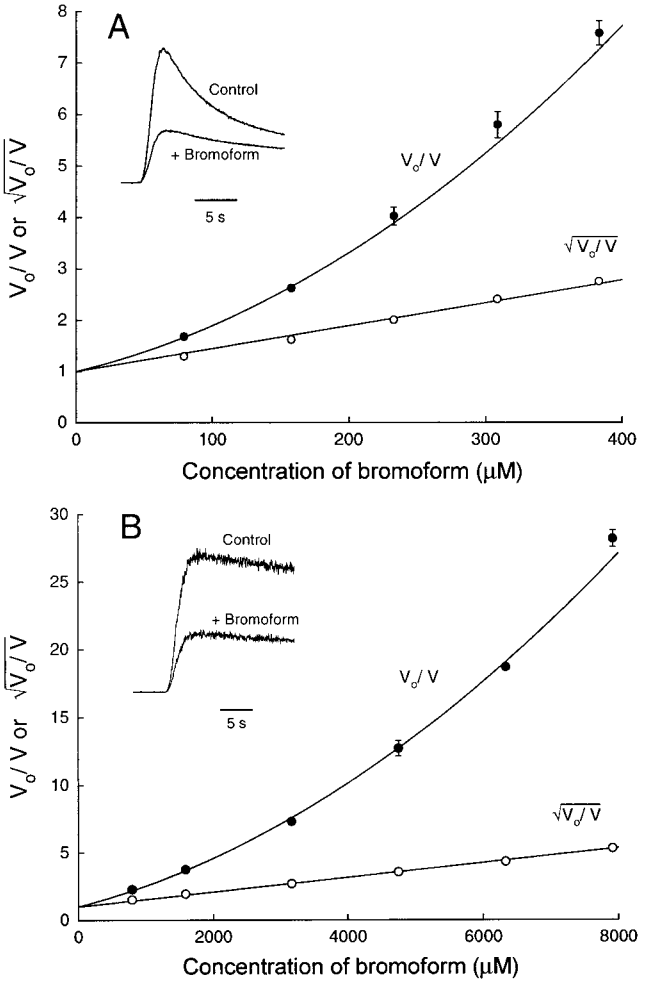

FIGURE 2 Inhibition of the firefly luciferase enzyme involves two molecules of bromoform. (*A*) Inhibition at high (2 mM) ATP. (*B*) Inhibition at low (2 μM) ATP. In both cases the luciferin concentration was 2 μM. Enzyme inhibition is expressed as a ratio of the control to the inhibited response (●) and as a square root of this ratio (○). Each data point represents the mean of at least three determinations; the error bars are standard errors of the mean. Where error bars are not shown they are smaller than the symbol. The lines are weighted (see Materials and Methods) least-squares fits to the data, constrained to go through unity on the ordinate axis. The ratio v_o/v is fit to a quadratic equation, whereas $\sqrt{v_0/v}$ is fit by a straight line. The insets show typical control and inhibited flashes with 160 μM bromoform for (*A*) and 800 μM bromoform for (*B*).

reduction), with the predominant effect being an increase in the apparent Michaelis constant K_m (from 180 ± 6 μM to 460 ± 30 μM luciferin). Although the noncompetitive element of the inhibition was small, we went on to characterize it in more detail by measuring the inhibition of the enzyme by bromoform at a concentration of luciferin that is large (1800 μM) compared to the luciferin K_m (180 μM at an ATP concentration of 2 μM). These data are shown in Fig. 4, where they are compared to the inhibition observed at a concentration of luciferin that is small (2 μM) compared to the luciferin K_m. It can be seen that the inhibition is greatly reduced and increases approximately linearly, rather than quadratically, when the luciferin concentration is increased from 2 to 1800 μM.

We determined the high-resolution structure of the luciferase enzyme in the presence of saturating concentrations of bromoform, but in the absence of ATP (despite extensive crystallization trials, we have been unable to obtain crystals of luciferase in its "high-ATP" form). From the x-ray diffraction data we calculated a difference electron density map (i.e., with and without bromoform) that clearly revealed the positions of two bromoform molecules binding to the enzyme (and three short loops of the polypeptide chain that had previously been omitted from the original structure). There was no evidence for any other bromoform-binding site. The final model included residues 3–198 and 201–544 and 351 water molecules (see Table 1 for the crystallographic statistics).

An overview of the structure is shown in Fig. 5 *A*. As previously described (Conti et al., 1996a), the enzyme consists of two domains: a large N-terminal domain and a smaller C-terminal domain that we believe move together to sandwich the luciferin and ATP substrates when they bind to the enzyme (we refer to the two conformations as the "low-ATP" and "high-ATP" forms of the structure). The two bromoform molecules lie close to one another and bind within pockets in the large N-terminal domain, causing minimal perturbations to the overall structure. A more detailed view of the binding environments is shown by the stereo representation in Fig. 5 *C*. One of the two anesthetic molecules is bound in a pocket that we can identify as the luciferin substrate-binding site (see Discussion), whereas the other is bound to a pocket accessible from the external surface of the enzyme and abuts the luciferin pocket. The binding environment of the bromoform molecule in the

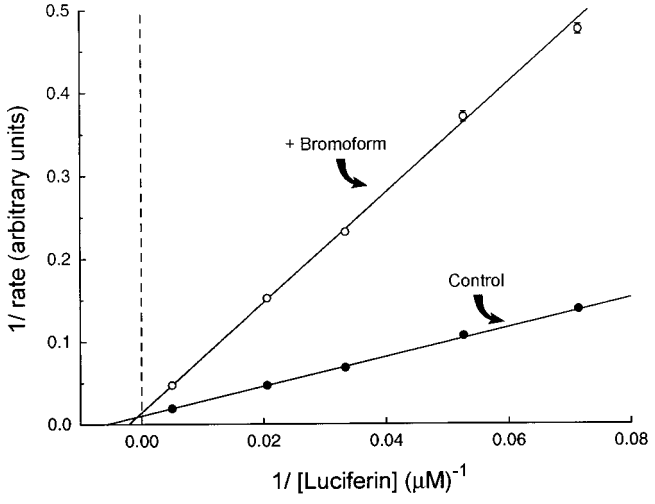

FIGURE 3 Anesthetic inhibition of firefly luciferase at a low ATP concentration (2 μM) is largely competitive with respect to luciferin. The reciprocal of the luciferase activity is plotted against the reciprocal of the luciferin concentration: ●, control; ○, 1600 μM bromoform. Each data point represents the mean of at least three determinations, and the error bars are standard errors of the mean. Where error bars are not shown they are smaller than the symbol. The straight lines were calculated using the method of weighted least squares (see Materials and Methods). For the control, K_m = 180 ± 6 μM luciferin and V_{max} = 100 ± 0.5. In the presence of 1600 μM bromoform, the apparent K_m = 460 ± 30 μM luciferin and V_{max} = 77 ± 3.

luciferin pocket is amphiphilic in nature, with one side of the anesthetic in close contact with apolar glycine and alanine residues (315 and 313, respectively), whereas the other side is coordinated by water molecules and two polar side chains: Arg^{218} and Glu^{311}. It also interacts with the aliphatic chain of Arg^{337}, which forms the "base" of the luciferin pocket. The bromoform in the "external" site is in a remarkably polar environment and makes specific interactions with two glutamic acids (311 and 354), Thr^{352}, His^{310}, and the guanidinium group of Arg^{337}. Although the overall structure of the N-terminal domain was little affected on anesthetic binding (the C_α carbon atoms could be superposed to give an rms difference of 0.21 Å), there were small realignments of some of the amino acid side chains that were in contact with the bromoform molecules. His^{310} was disordered in the original structure, but the presence of a bromoform molecule has provided a sufficiently strong interaction so that clear density for the histidine side chain appeared when the anesthetic molecules bound. Similarly, the carboxylate moieties of the two glutamic acid side chains (311 and 354) both move slightly to coordinate the bromoform molecules. The only other change in the enzyme structure on anesthetic binding is a conformational change in the aliphatic chain of Arg^{337}, although the guanidinium group itself remains in a similar position.

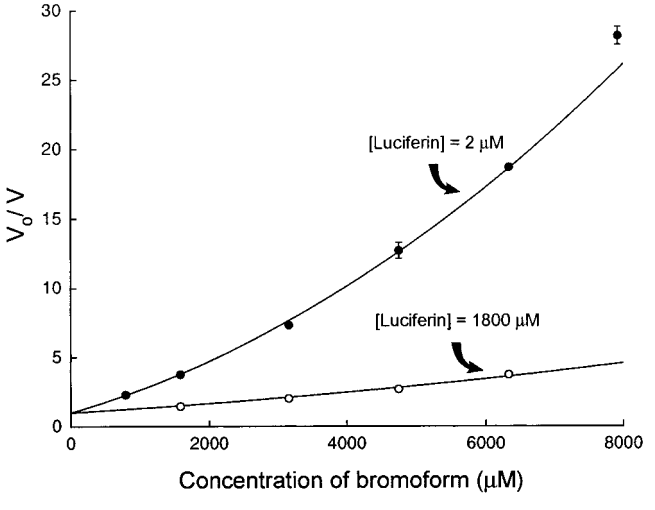

FIGURE 4 The inhibition observed when the luciferin concentration is small (2 μM) compared to the luciferin K_m (180 μM) increases quadratically, whereas the inhibition is greatly reduced and increases approximately linearly when the luciferin concentration is large (1800 μM) compared to the luciferin K_m. In both cases the ATP concentration was 2 μM. The lines are calculated using the model described in the discussion. See text for details.

DISCUSSION

Although it is known that bromoform has sedative properties (IARC, 1991), its anesthetic potency has not, to our knowledge, been determined. Its EC_{50} concentration of 185 μM for inducing a loss of righting reflex in tadpoles (Fig. 1) is close to that which could have been predicted from its physical properties (octanol/water partition coefficient $\log_{10} P_{oct}$ = 2.38, aqueous solubility C_{sat} = 11.9 mM, IARC (1991)), or its ability to inhibit the high-ATP form of the firefly luciferase enzyme (see Fig. 2 *A*). By these measures it can therefore be considered to be an unexceptional general anesthetic and has an anesthetic potency and physical properties similar to those of the inhalational agent halothane ($\log_{10} P_{oct}$ = 2.30; C_{sat} = 17.5 mM, and tadpole EC_{50} = 230 μM; Firestone et al., 1986; Raventós, 1956).

The inhibition of the firefly luciferase enzyme by bromoform also followed a familiar pattern (Franks and Lieb, 1984), with two molecules of the anesthetic being involved in the inhibition, and this inhibition being greater at high, rather than low, concentrations (Moss et al., 1991) of the substrate ATP (see Fig. 2). Because we could only obtain crystals of the enzyme in the absence of ATP, we mainly studied the effects of bromoform on enzyme activity at a very low ATP concentration (2 μM). Under these conditions, the inhibition was predominantly competitive (Fig. 3), although there was also a small degree of noncompetitive inhibition. This was made more apparent when the inhibition was measured with the luciferin binding site effectively saturated (by using a luciferin concentration 10 times greater than its K_m). This showed that a single, relatively weakly binding, bromoform molecule was responsible for the noncompetitive component, because with the luciferin site saturated, the inhibition increased roughly linearly with bromoform concentration (Fig. 4).

Therefore, the simplest model that fits our inhibition data is one in which there is a single, relatively high-affinity site to which bromoform binds in competition with the luciferin substrate, and a weaker noncompetitive site that binds independently of the luciferin concentration. An equilibrium scheme describing this model is shown below:

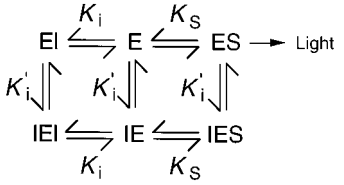

where the luciferase enzyme E, luciferin substrate S, and bromoform inhibitors I are shown at equilibrium with their various complexes; K_S is the luciferin dissociation constant; K_i is the dissociation constant for the competitive bromoform molecule; and K'_i is the dissociation constant for the noncompetitive bromoform molecule.

It is straightforward to show that, according to this scheme, the rate of the luciferase reaction v is given by

$$v = \frac{V_{max} S}{\left[S + K_S\left(1 + \frac{I}{K_i}\right)\right]\left[1 + \frac{I}{K'_i}\right]} \quad (2)$$

where V_{max} is the maximum rate of the reaction and S is the luciferin concentration. Hence the ratio of rates in the absence (v_o) and presence (v) of bromoform is given by

$$\frac{v_0}{v}(S, I) = \frac{\left[S + K_S\left(1 + \frac{I}{K_i}\right)\right]\left[1 + \frac{I}{K'_i}\right]}{S + K_S} \quad (3)$$

When this equation is fitted to the data of Fig. 4 with both S and I as independent variables, excellent agreement is obtained, with this simple model accounting for the data at both high and low luciferin concentrations. The best fit to the data gives values for the competitive and noncompetitive dissociation constants of 790 ± 30 μM and 5800 ± 400 μM, respectively.

What are the molecular architectures of these anesthetic binding sites? The crystal structure that we have determined was under conditions that would have strongly favored the IEI complex in the above scheme. The two bromoform molecules were immediately apparent in the structure, with unambiguous and well-defined electron densities (Fig. 5 *C*). The anesthetic molecules evidently bind to the enzyme in preformed pockets, much as we had anticipated some years ago (Franks and Lieb, 1984, 1985). There is no generalized or even local disordering of the structure. Indeed, the only small rearrangements are local ordering or slight realignments of certain amino acid residues. The old suggestion (Ueda and Kamaya, 1973) that general anesthetics inhibit the firefly luciferase enzyme by disordering its structure is clearly incorrect.

One of the two bromoform molecules can be readily identified as the competitive inhibitor (*magenta* in Fig. 5) because it binds in a pocket on the enzyme that has been tentatively identified as the luciferin-binding site by analogy with the substrate-binding site on the structurally related enzyme, gramicidin synthetase (Conti et al., 1997). This bromoform molecule binds within a cavity that has both polar and apolar characteristics, with water and polar residues on one side and apolar residues on the other. Although we expected to see anesthetic molecules binding to an amphiphilic pocket on the protein (Franks and Lieb, 1985), and anticipated that this would also form a part of the luciferin-binding site (Moss et al., 1991), we did not expect to see an additional, and strikingly polar, anesthetic-binding pocket (containing the *yellow* bromoform molecule in Fig. 5, *A* and *C*). This binding site presumably accounts for the weak noncompetitive component of the inhibition. Although this site only provides a relatively weak binding environment for bromoform, it does show that polar interactions can orient and order anesthetic molecules with large polarizable atoms such as bromine. This has previously been observed for the binding of dichloroethane to insulin (Gursky et al., 1994).

The structure we have determined is the "low-ATP" form of the enzyme that binds anesthetics, including bromoform, less tightly than the "high-ATP" form (see Fig. 2 and Moss et al., 1991). What can be learned from our structure about the molecular basis for this changing anesthetic affinity? Until we have determined the luciferase structure in its "high-ATP" form, we cannot draw definitive conclusions; nonetheless, a great deal can be inferred from a comparison with gramicidin synthetase, the structure of which has been determined in its "high-ATP" form (Conti et al., 1997). This enzyme catalyzes a reaction analogous to that of firefly luciferase, except that the firefly luciferin substrate is replaced by phenylalanine, and a phenylalanine-AMP adenylate is formed, rather than a luciferyl-AMP adenylate. Despite a sequence identity of only 16% (Conti et al., 1997), the two enzymes are closely related structurally, with N- and C-terminal domains of similar topologies in the two proteins, and with domain structures that superimpose with an rms deviation of the main-chain α-carbon atoms of less than 1.5 Å (for all atoms within 3 Å). The main difference between the structures is that the gramicidin synthetase enzyme was crystallized in the presence of ATP and the N- and C-terminal domains have come together, sandwiching the substrates.

A comparison between the "low-ATP" luciferase structure and the "high-ATP" gramicidin synthetase structure shows that, in addition to the relative movement of the N- and C-terminal domains, a loop of main chain (residues 314–319) moves several Ångstroms on ATP binding (see Fig. 5 *B*). In the low-ATP structure this loop hinders substrate (luciferin or phenylalanine) binding by constricting one dimension of the binding pocket. However, in the high-ATP structure, the loop has moved so as to form a cavity large enough to bind the substrate. We can therefore suppose that this will also provide space for the binding of a second competitive anesthetic molecule. Interestingly,

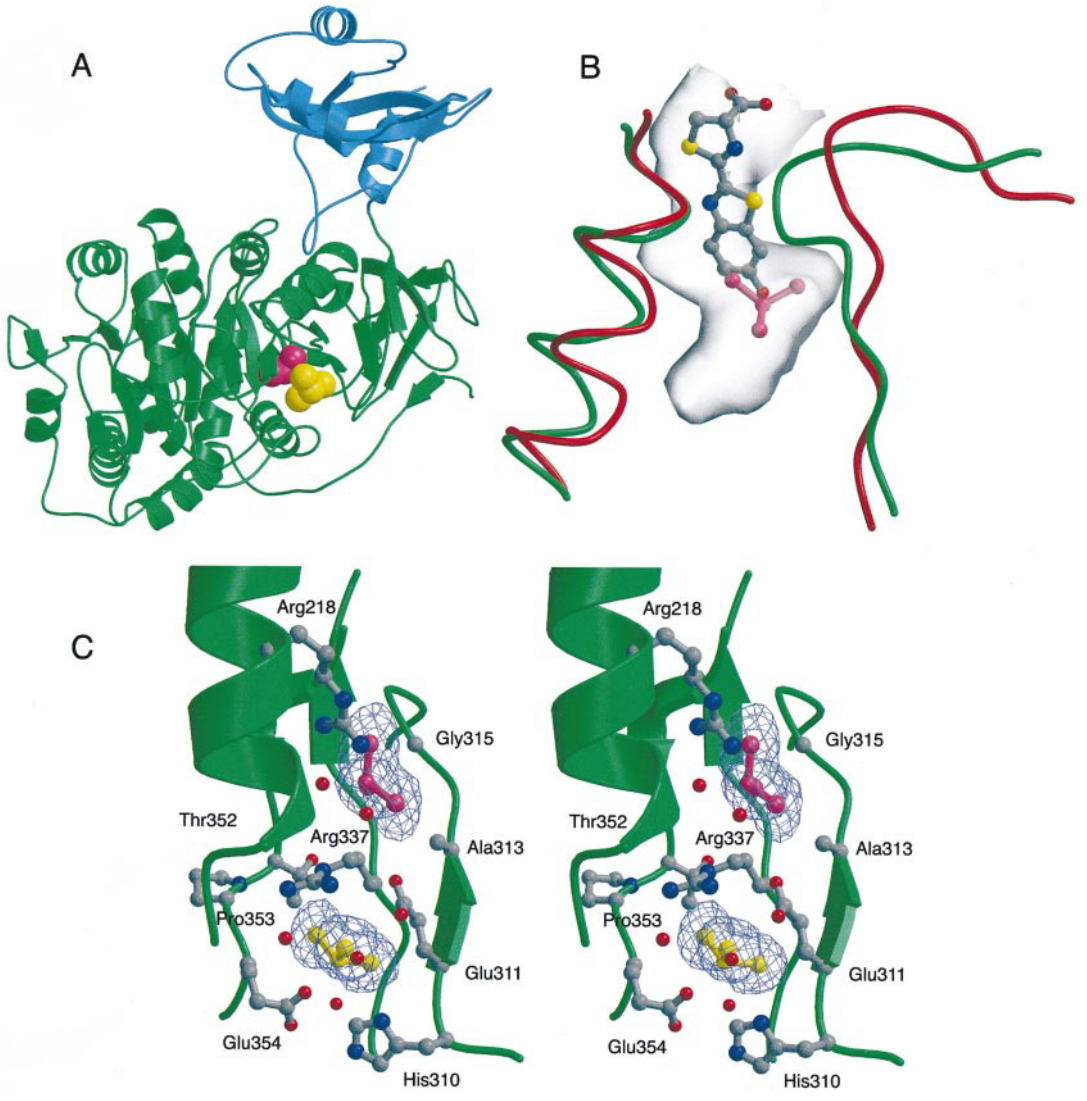

FIGURE 5 Two molecules of bromoform bind to the luciferase enzyme. (*A*) Ribbon representation of the firefly luciferase molecule showing the large N-terminal domain (residues 4–437) in green and the smaller C-terminal domain (residues 438–544) in blue. The bromoform molecule that binds in the luciferin-binding pocket is shown in magenta, and the bromoform molecule that binds to an "external" polar pocket is shown in yellow. (*B*) The structural basis for the enhanced anesthetic sensitivity of the luciferase enzyme at high ATP concentrations. The diagram compares the conformation of the polypeptide backbone of the "low-ATP" firefly luciferase structure (*green*) with that of gramicidin synthetase (*red*), which was cocrystallized in the presence of high concentrations of ATP (Conti et al., 1997). The position of the competitive bromoform molecule (shown in *magenta*) in the firefly luciferase binding pocket (*gray shading*) is illustrated. The diagram shows the position of the substrate firefly luciferin deduced from the position of its analogous substrate (phenylalanine) in the crystal structure of gramicidin synthetase. (*C*) Stereo diagram showing the amino acid residues of firefly luciferase that are within 4 Å of the two bound bromoform molecules. The water molecules are shown as isolated red spheres. The bromoform molecules are each contained within defined pockets or cavities in the protein. The diagram includes difference electron density (in *blue*) contoured at 4σ with the anesthetic molecules omitted from the model. The figure was generated using Raster3D (Merritt and Bacon, 1997) and Molscript (Kraulis, 1991), with modifications by R. Esnouf (1997).

with halothane, two molecules bind to the luciferase enzyme in its high-ATP form, whereas only a single molecule binds at low ATP, an observation entirely consistent with this picture (Moss et al., 1991).

However, the binding of a second competitive molecule with the same affinity as the first is not sufficient to explain the enhanced anesthetic sensitivity at high ATP concentrations. In the case of bromoform, the two competitive molecules in the high-ATP form would have to bind significantly more tightly than the single competitive molecule in the low-ATP form to account for the increased inhibition observed at high ATP concentrations. An explanation for the enhanced anesthetic sensitivity is likely to lie in the fact that, when ATP binds to the enzyme and the two domains of the protein come together, the anesthetic molecules binding within the luciferin-binding pocket are trapped, effectively enhancing their apparent binding affinities. The same mechanism would also account for the increased affinity of luciferin observed at high concentrations of ATP (Moss et al., 1991).

Although the structure of the high-ATP form of the luciferase enzyme will be needed before we can confidently explain its remarkable ability to bind such a diverse range of general anesthetics, certain clear conclusions can be drawn from the present study. Anesthetics exert their effects by binding to preformed pockets on the protein with minimal perturbations to the overall structure. The main anesthetic-binding site that accounts for the inhibition is the luciferin-binding pocket itself, and the competitive nature of the inhibition has a straightforward molecular explanation. This binding site is amphiphillic, with both polar and apolar characteristics. When ATP binds to the enzyme, the luciferin-binding site increases in size, and its exit becomes occluded. This provides a explanation for the enhanced anesthetic binding at high ATP concentrations.

We thank the Medical Research Council (UK) for support.

REFERENCES

Abraham, M. H., W. R. Lieb, and N. P. Franks. 1991. Role of hydrogen bonding in general anesthesia. *J. Pharm. Sci.* 80:719–724.

Brünger, A. T. 1992. The free R value: a novel statistical quantity for assessing the accuracy of crystal structures. *Nature.* 355:472–474.

Brünger, A. T., J. Kuriyan, and M. Karplus. 1987. Crystallographic *R*-factor refinement by molecular-dynamics. *Science.* 235:458–460.

CCP4. 1994. The CCP4 suite: programs for protein crystallography. *Acta Crystallogr. D.* 50:760–767.

Conti, E., N. P. Franks, and P. Brick. 1996a. Crystal structure of firefly luciferase throws light on a superfamily of adenylate-forming enzymes. *Structure.* 4:287–298.

Conti, E., L. F. Lloyd, J. Akins, N. P. Franks, and P. Brick. 1996b. Crystallization and preliminary diffraction studies of firefly luciferase from *Photinus pyralis. Acta Crystallogr. D.* 52:876–878.

Conti, E., T. Stachelhaus, M. A. Marahiel, and P. Brick. 1997. Structural basis for the activation of phenylalanine in the non-ribosomal biosynthesis of gramicidin S. *EMBO J.* 16:4174–4183.

Dickinson, R., N. P. Franks, and W. R. Lieb. 1993. Thermodynamics of anesthetic/protein interactions. Temperature studies on firefly luciferase. *Biophys. J.* 64:1264–1271.

Esnouf, R. M. 1997. An extensively modified version of Molscript that includes greatly enhanced coloring capabilities. *J. Mol. Graph.* 15: 133–138.

Firestone, L. L., J. C. Miller, and K. W. Miller. 1986. Tables of physical and pharmacological properties of anesthetics. *In* Molecular and Cellular Mechanisms of Anesthetics. S. H. Roth and K. W. Miller, editors. Plenum, New York. 455–470.

Forman, S. A., K. W. Miller, and G. Yellen. 1995. A discrete site for general anesthetics on a postsynaptic receptor. *Mol. Pharmacol.* 48: 574–581.

Franks, N. P., and W. R. Lieb. 1978. Where do general anaesthetics act? *Nature.* 274:339–342.

Franks, N. P., and W. R. Lieb. 1982. Molecular mechanisms of general anaesthesia. *Nature.* 300:487–493.

Franks, N. P., and W. R. Lieb. 1984. Do general anaesthetics act by competitive binding to specific receptors? *Nature.* 310:599–601.

Franks, N. P., and W. R. Lieb. 1985. Mapping of general anaesthetic target sites provides a molecular basis for cutoff effects. *Nature.* 316:349–351.

Franks, N. P., and W. R. Lieb. 1994. Molecular and cellular mechanisms of general anaesthesia. *Nature.* 367:607–614.

Gursky, O., E. Fontano, B. Bhyravbhatla, and D. L. D. Caspar. 1994. Stereospecific dihaloalkane binding in a pH-sensitive cavity in cubic insulin crystals. *Proc. Natl. Acad. Sci. USA.* 91:12388–12392.

Hansch, C., A. Vittoria, C. Silipo, and P. Y. C. Jow. 1975. Partition coefficients and the structure-activity relationship of the anesthetic gases. *J. Med. Chem.* 18:546–548.

IARC. 1991. *IARC Monogr. Eval. Carcinog. Risks Hum.* 52:213–242.

Kraulis, P. J. 1991. MOLSCRIPT: a program to produce both detailed and schematic plots of protein structures. *J. Appl. Crystallogr.* 24:946–950.

McElroy, W. D., and H. H. Seliger. 1961. Mechanisms of bioluminescent reactions. *In* Light and Life. W. D. McElroy and B. Glass, editors. The Johns Hopkins University Press, Baltimore. 219–257.

Merritt, E. A., and D. J. Bacon. 1997. Raster3D: photorealistic molecular graphics. *Methods Enzymol.* 227:505–524.

Mihic, S. J., Q. Ye, M. J. Wick, V. V. Koltchine, M. D. Krasowski, S. E. Finn, M. P. Mascia, C. F. Valenzuela, K. K. Hanson, E. P. Greenblatt, R. A. Harris, and N. L. Harrison. 1997. Sites of alcohol and volatile anaesthetic action on $GABA_A$ and glycine receptors. *Nature.* 389: 385–389.

Miller, K. W. 1985. The nature of the site of general anesthesia. *Int. Rev. Neurobiol.* 27:1–61.

Moss, G. W. J., N. P. Franks, and W. R. Lieb. 1991. Modulation of the general anesthetic sensitivity of a protein: a transition between two forms of firefly luciferase. *Proc. Natl. Acad. Sci. USA.* 88:134–138.

Raventós, J. 1956. The action of fluothane—a new volatile anaesthetic. *Br. J. Pharmacol. Chemother.* 11:394–410.

Sandorfy, C. 1978. Intermolecular interactions and anesthesia. *Anesthesiology.* 48:357–359.

Schoenborn, B. P. 1976. Dichloromethane as an antisickling agent in sickle cell hemoglobin. *Proc. Natl. Acad. Sci. USA.* 73:4195–4199.

Schoenborn, B. P., H. C. Watson, and J. C. Kendrew. 1965. Binding of xenon to sperm whale myoglobin. *Nature.* 207:28–30.

Taheri, S., M. J. Halsey, J. Liu, E. I. Eger, II, D. D. Koblin, and M. J. Laster. 1991. What solvent best represents the site of action of inhaled anesthetics in humans, rats, and dogs? *Anesth. Analg.* 72:627–634.

Tomlin, S. L., A. Jenkins, W. R. Lieb, and N. P. Franks. 1998. Stereoselective effects of etomidate optical isomers on gamma-aminobutyric acid type A receptors and animals. *Anesthesiology.* 88:708–717.

Ueda, I., and H. Kamaya. 1973. Kinetic and thermodynamic aspects of the mechanism of general anesthesia in a model system of firefly luminescence in vitro. *Anesthesiology.* 38:425–436.

Waud, D. R. 1972. On biological assays involving quantal responses. *J. Pharmacol. Exp. Ther.* 183:577–607.